Molecular Neurobiology

ISSN0893-7648/94/8(1): 41–48/$3.00

Familial Gerstmann-Sträussler-Scheinker Disease with Neurofibrillary Tangles

Bernardino Ghetti,*[,1] F. Tagliavini,[2] G. Giaccone,[2] O. Bugiani,[2] Blas Frangione,[3] M. R. Farlow,[3] and S. R. Dlouhy[3]

[1]*Indiana University School of Medicine, Indianapolis, IN;* [2]*Istituto Neurologico "Carlo Besta," Milano, Italy; and* [3]*New York University Medical Center, New York, NY*

Abstract

Patients affected with Gerstmann-Sträussler-Scheinker disease from two families, one from Indiana and one of Swedish origin, have been studied. The patients are clinically characterized by cerebellar ataxia, extrapyramidal signs, and dementia. Accumulation of amyloid deposits and neurofibrillary tangles are the most conspicuous neuropathologic features. In the patients from the Indiana family, the amyloid contains an 11-kDa peptide, an amyloidogenic degradation product of the prion protein. The neurofibrillary tangles are composed of paired helical filaments and immunoreact with antibody to A68, an abnormally phosphorylated form of the microtubule-associated protein τ. In these families, the disease is caused by a point mutation in the PRNP gene. In the Indiana family, the mutation is at codon 198, and in the Swedish family at codon 217.

Index Entries: Gerstmann-Sträussler-Scheinker disease; prion protein; amyloid; neurofibrillary tangles.

Introduction

Gerstmann-Sträussler-Scheinker disease (GSS), a familial neurodegenerative disorder, is characterized clinically by ataxia, extrapyramidal signs, and adult-onset dementia, and neuropathologically by multicentric amyloid plaques in the cerebrum and cerebellum *(1–3)*. The amyloid deposits in GSS are immunoreactive to antisera raised against the prion protein (PrP) 27–30, a proteinase-K-resistant peptide of 27–30 kDa derived by limited proteolysis from an abnormal 33–35 kDa isoform of a neuronal sialoglycoprotein designated PrP^{Sc} *(4)*. Point mutations at codons 102, 105, 117, 198, and 217, and an insert mutation between codons 51 and 91 of the human PRNP gene located on the short arm of chromosome 20, have been described in different pedigrees of GSS *(5–16)*. The point mutations at codon 198 (GSS-198, identified in an Indiana kindred) *(14,16)* and codon 217 (GSS-217, identified in a family of Swedish origin) *(16)* appear to result in a disease that is phenotypically distinct from those caused by the other PRNP mutations. In GSS-198 and GSS-217, in addition to the presence of multicentric amyloid plaques characteristic of GSS, there are also numerous Alzheimer-type neurofibrillary tangles *(15,17,18)*. Clinical, neuropathological, biochemical, and molecular genetic features of these two forms of GSS are reviewed in this article.

*All correspondence and reprint requests should be addressed to: B. Ghetti, Indiana University, 635 Barnhill Dr., Indianapolis, IN 46202-5120.

Clinical Features

GSS-198

Gerstmann-Sträussler-Scheinker disease has been studied in an Indiana family for the past 16 yr. The pedigree has been traced back to the year 1792. In patients from this kindred, onset of symptoms varies from the 40s to the early 60s *(15,19)*. Initial symptoms are a gradual loss of short-term memory and progressive clumsiness in walking, exaggerated or first noticed when the individual is under stress. Early signs of cognitive impairment and eye movement abnormalities may be detected by specific tests before clinical onset of symptoms *(20)*. Later, there is increasing difficulty with gait, bradykinesia, rigidity, and dysarthria. Symptoms may progress slowly over 5 yr or rapidly over as little as 1 yr. Rigidity, bradykinesia, and dementia worsen late in the disease. Psychotic depression has been seen in several patients. Tremor is mild or absent. Without carbidopa/levodopa treatment, rapid weight loss and death usually occur within 1–4 yr of onset of Parkinsonism. Bradykinesia and rigidity improve with treatment; however, death still occurs from pneumonia or other illness. The total duration of disease from initial onset of symptoms varies from 2 to 11 yr. In the last stage, patients have severe extrapyramidal abnormalities, dysphagia, and global dementia.

GSS-217

Gerstmann-Sträussler-Scheinker disease in a family of Swedish origin has been studied over the past 3 yr. Clinical information is available on only two siblings. The first patient, a 47-yr-old female, had an episode of mania and depression. At age 62, she experienced difficulty with memory and with motor coordination. Her memory deteriorated over the course of 5 yr. Ataxia became more prominent to the point that she needed support while walking. Over the last 12 mo of her life, she could not take care of herself. She died at age 67.

The second patient, a 66-yr-old male, developed auditory hallucinations and weight loss. Symptoms improved with an antidepressant medication. A computerized tomogram of the head revealed mild cerebral atrophy with focal predominance in the region of the left Sylvian fissure. Two years later, he developed mania that was controlled with lithium and neuroleptic medication. Mental status deteriorated despite treatment, and he showed increasing Parkinsonian signs and dementia. The patient died at age 72.

Neuropathology

The central nervous systems of eight GSS-198 patients and one nonsymptomatic GSS-198 gene carrier and two GSS-217 patients have been studied *(17,18,21–23)*. Affected subjects consistently show moderate cerebral atrophy and moderate to severe cerebellar atrophy. Other main macroscopic findings are loss of pigment of both the substantia nigra and the locus ceruleus.

Microscopically, the following lesions are observed: amyloid deposits with or without a neuritic component (Figs. 1A,B, 2A,B), neurofibrillary tangles (Fig. 3A,B), nerve cell loss gliosis, and iron deposition. Spongiform changes are inconspicuous in GSS-198 and GSS-217.

Nerve cell loss is recognizable in cortical regions. In the cerebellar cortex, rarefaction of Purkinje cells is severe; swollen axons of Purkinje cells are found in the granule cell layer. Neuronal loss is also evident in the red nucleus, substantia nigra, dentate nucleus, and inferior olivary nucleus. Iron deposition is prominent in globus pallidus, caudate nucleus, putamen, red nucleus, and substantia nigra of GSS-198 patients.

A neurologically asymptomatic subject, later found to be a carrier of the 198 mutation, died suddenly at age 42. Amyloid deposits in focal areas of the cerebellar molecular and granule cell layers were already prominent. Amyloid deposits were occasionally found in the neocortex. The amyloid deposits were immunolabeled by antibody to PrP. Neurofibrillary tangles were rarely found in the cerebral cortex.

Amyloid in GSS-198 and GSS-217

In all affected individuals, amyloid deposits are distributed throughout the gray structures of the cerebrum, cerebellum, and midbrain. They are intertwined at the periphery with astrocytic processes. Microglial elements and macrophages are present. The diameter of the amyloid deposits ranges between 10 and 100 μm in the cerebellum, and between 15 and 160 μm in the cerebral cortex. One or more amyloid cores are observed in each plaque. In thioflavine-S-treated sections, amyloid deposits are strongly fluorescent when observed under UV light. Fluorescent deposits are not seen in or around the walls of blood vessels; however,

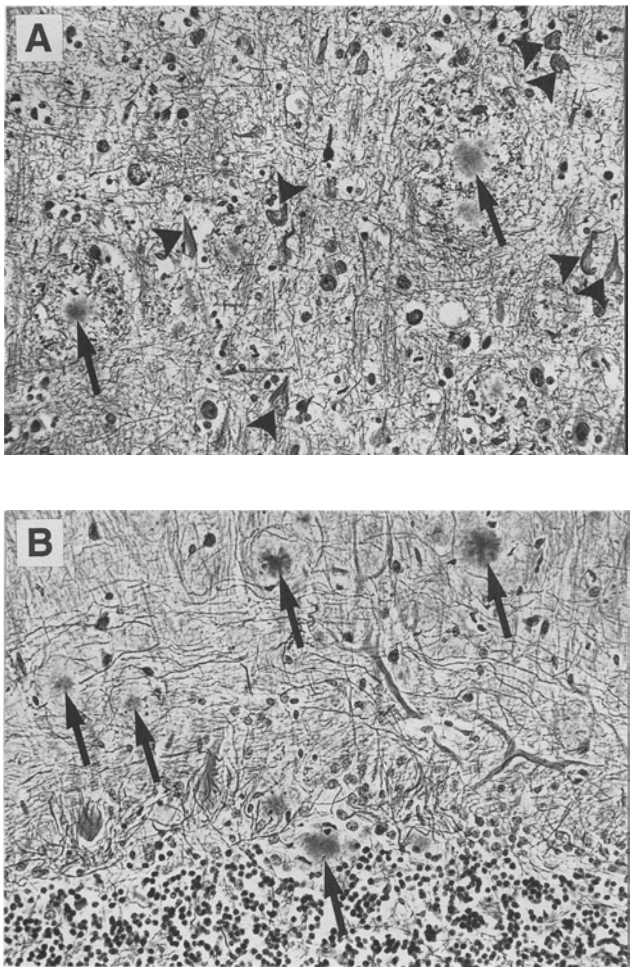

Fig. 1. **(A)** Amyloid deposits (arrows) and neurofibrillary tangles (arrowheads) in the cerebral cortex of a GSS-198 patient. Bodian stain, ×250. **(B)** Amyloid deposits (arrows) in the molecular layer and granule cell layer of the cerebellar cortex of a GSS-198 patient. Bodian stain, ×250.

they may be present in the parenchyma adjacent to vessels. In the cerebral cortex, the highest concentration of amyloid deposits of any type is found in layers four, five, and six; however, deposits in clusters are often found in subpial regions of the cerebral and cerebellar cortex.

In the cerebral cortex, amyloid deposits are in most instances associated with a crown of degenerating neurites (Figs. 1A, 2A), so that when these lesions are studied with classical stains, they are morphologically very similar to the neuritic plaques of Alzheimer's disease (AD). In the neocortex, a severe involvement is seen in the frontal, insular, temporal, and parietal cortex. A less severe involvement is seen in the occipital cortex. A moderate involvement is seen in the hippocampal formation. Of the subcortical nuclei, the claustrum, the globus pallidus, and the thalamus are more involved than the caudate and putamen. The mesencephalic tegmentum, the substantia nigra, and periaqueductal gray matter are severely involved. The average diameter of the amyloid plaques is greatest in the neocortex, anterior, and dorsolateral thalamic nuclei, and least in the basal ganglia, ventrolateral thalamic nucleus, and midbrain. There is moderately severe amyloid deposition in the anterior, dorsomedial, ventrolateral, and lateral dorsal nuclei of the thalamus. The hippocampal plaques occur predominantly within the stratum lacunosum-moleculare of the CA1 sector and subiculum, with relative sparing of the CA2 sector and end folium. Numerous Hirano bodies are present in the hippocampal formation.

In the cerebellum, amyloid deposits (Figs. 1B, 2B) are most numerous in the molecular layer, but are also occasionally present within the granule cell layer and subcortical white matter.

By electron microscopy, the amyloid deposits appear to be composed of bundles of fibrillar structures, measuring 9–10 nm, and radiating out from a central core. Surrounding the mass of fibrils, neuritic processes are found in the cerebral cortex, but are generally absent in the cerebellum.

Immunohistochemistry of Amyloid

The cerebral and cerebellar amyloid deposits, with and without a neuritic component, are immunoreactive with antisera raised against the protease-resistant core of the prion protein (PrP) designated PrP 27–30 (Fig. 2B). Immunolabeling with anti-PrP antisera is not detected in the vessel wall; however, immunolabeled deposits are occasionally found adjacent to the Virchow-Robin spaces.

Two types of anti-PrP immunoreactivity are detected in gray structures of GSS patients who were carriers of either the 198 or 217 mutation: (1) amyloid deposits and (2) deposits without tinctorial and optical properties of amyloid. Amyloid deposits are revealed by thioflavine-S and are labeled by an antiserum directed to residues 90–102 of the cDNA-deduced amino acid sequence of human PrP. In sections treated with formic acid, the amyloid cores are strongly labeled, whereas the surrounding tissue is faintly decorated. When antisera to the C-terminal (residues 220–231) and N-terminal (residues 23–40) domains of human PrP are

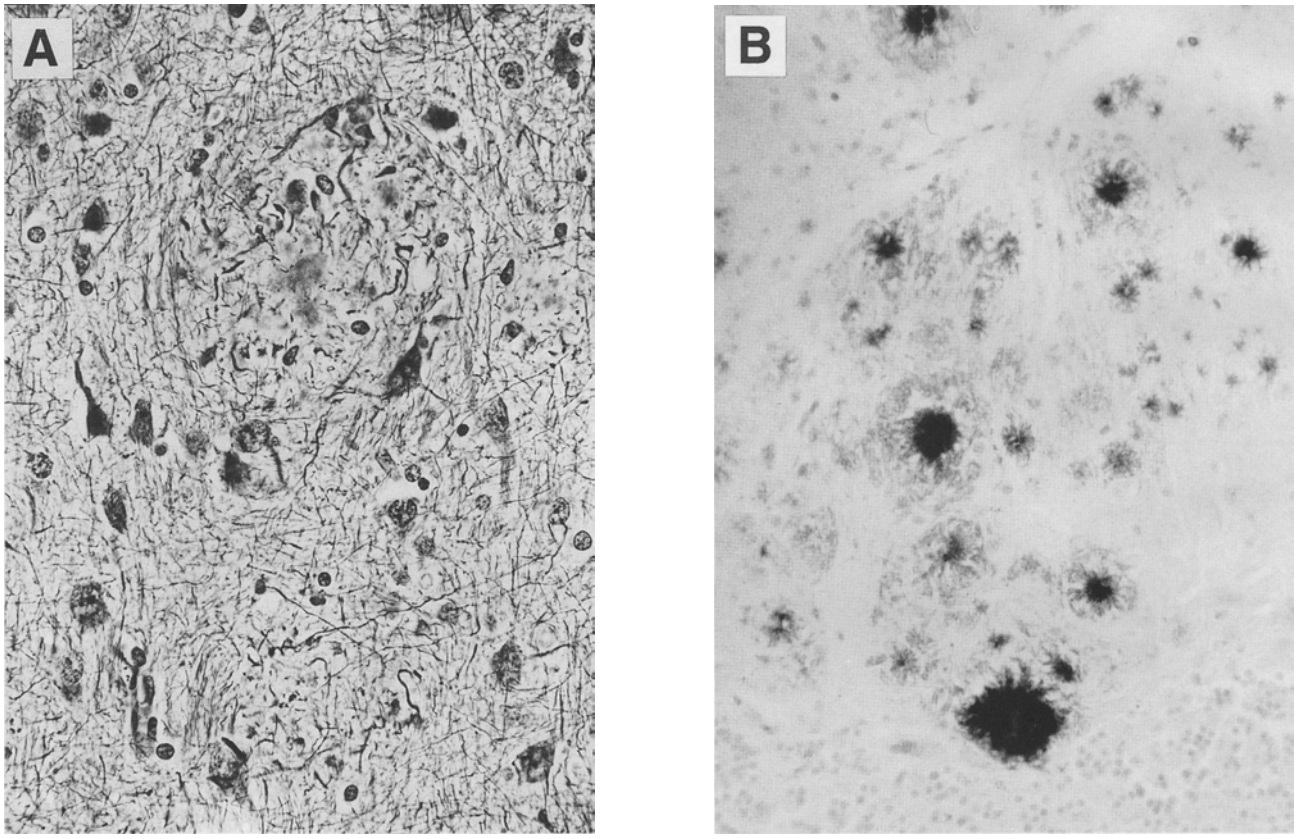

Fig. 2. **(A)** Amyloid deposit surrounded by abnormal neurites in the cerebral cortex of a GSS-198 patient. Bodian stain, ×400. **(B)** Amyloid deposits in the cerebellar molecular layer of a GSS-198 patient. Anti-PrP immunolabeling. ×250.

used, the amyloid cores are not labeled; however, a ring of immunopositivity is observed around the cores. These data are in agreement with studies carried out with antisera to the C- and N-terminal domains of the hamster PrP (22). In many instances, unstained cores are surrounded by a sharply defined ring of intense immunoreactivity.

In the cerebral cortex, the amyloid deposits are surrounded by numerous neuritic elements. By immunohistochemistry, the neurites are labeled by Alz50, a monoclonal antibody to a 68-kDa protein present in the brain of Alzheimer's patients, anti-ubiquitin, antisynaptophysin, and antipreA4, a monoclonal for an epitope between residues 60 and 100 of the amyloid precursor protein (βPP). In a 73-yr-old patient carrying the 198 mutation and in one patient carrying the 217 mutation, a crown of anti-β(A4) immunopositivity is seen around areas of anti-PrP immunopositivity. For the second patient carrying the 217 mutation, insufficient tissue was available to carry out immunohistochemical studies. Immunoreactivity with anti-β(A4) protein associated or nonassociated with anti-PrP immunopositivity is seen in the neocortex, basal ganglia, thalamus, and cerebellar cortex in the patient carrying the 198 mutation. In the patient carrying the 217 mutation, most anti-β(A4) protein immunopositivity is seen in association with anti-PrP immunopositivity; the most affected areas are neocortex, amygdala, substantia innominata, and thalamus.

Fibrillary astrocytes surrounding the amyloid deposits are demonstrated by GFAP immunohistochemistry. Individual plaques contain numerous microglial cells immunohistochemically demonstrated with antiferritin antibody.

Electron Microscopy

The amyloid deposits are composed of radially arranged fibrils with a diameter of 10 nm. The vast majority of the cerebellar amyloid deposits did not

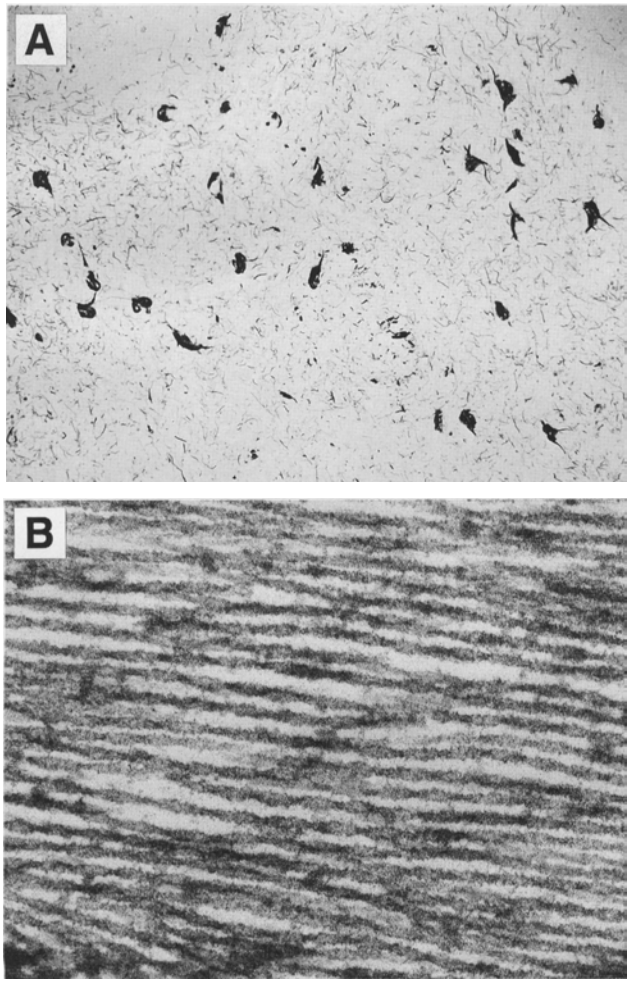

Fig. 3. **(A)** Neurofibrillary tangles in the cerebral cortex of a GSS-198 patient. Gallyas stain, ×160. **(B)** Paired helical filaments constitute the neurofibrillary tangles in a GSS-217 patient. ×100,000.

have any associated neurites. In many instances, abnormal neurites are seen around neocortical amyloid deposits.

In studies carried out by electron microscopy in patients with the 198 mutation, antiserum to a peptide corresponding to residues 90–102 of hamster PrP decorated 8–10 nm fibrils in the amyloid core, whereas antisera to synthetic peptides corresponding to residues 15–40 and 220–232 of hamster PrP label material at the periphery of the cores.

Biochemistry of Amyloid in GSS-198

Amyloid cores have been isolated from cerebral cortex and basal ganglia of two patients carrying the 198 mutation *(24)*. Proteins were extracted with formic acid and fractionated by gel filtration. Two major peaks were obtained: the void volume (fraction 1) and a peak centered at 11 kDa on SDS-PAGE (fraction 6). Moreover, four minor intermediate peaks (fractions 2–5) and a lower molecular-weight peak were present in the chromatograms. These fractions have been subjected to immunoblot analysis using an antiserum to PrP 27–30, purified from scrapie-infected hamster brain, and four antisera to synthetic peptides corresponding to residues 15–40, 90–102, 142–172, and 220–232 of cDNA-deduced amino acid sequence of hamster PrP, respectively. The immunochemical analysis shows that the 11-kDa peptide, the major constituent of the amyloid extract, is strongly labeled by the antiserum to PrP 27–30 and by the peptide raised against residues 90–102; conversely, it is weakly detected by the antisera against residues 140–172, and is nonreactive with antisera against residues 15–40 and 220–232. The data suggest that the amyloid protein is an internal fragment of PrP. In addition, higher molecular-weight species of PrP-related peptides with apparently intact N-termini are present in fractions 2–5. The 11-kDa amyloid protein has been further purified by HPLC and aliquots digested with endoproteinase Lys-C. Automated sequence analysis of the intact 11-kDa peptide and of peptides generated by enzymatic digestion shows that the amyloid protein has a N-terminal lysine corresponding to codon 58 of the amino acid sequence deduced from human PrP cDNA, and appears to end at codon 150. Studies are in progress to characterize further the amyloid of GSS-198 and GSS-217 patients.

Neurofibrillary Tangles in GSS-198 and GSS-217

In all the patients with codon 198 and 217 mutations, numerous neurofibrillary tangles are observed in the neocortex (Fig. 3A,B) and several subcortical structures *(15,17,18,21–24)*. Cortical regions particularly rich in neurofibrillary tangles are the frontal, cingulate, parietal, insular, and parahippocampal cortex, where neurons of layer five are most involved. In the parahippocampal cortex, layer two is also severly involved. In the remaining cortical regions, neurofibrillary tangles are present, but less numerous. In the hippocampus, neurofibrillary tangles are not found in the CA1 through CA3 areas, but may be present in CA4. The subcortical nuclei show a variable degree of involvement with tangles, the nucleus basalis being severely involved in patients with GSS-198. In mid-

brain and pons, the substantia nigra, the griseum centrale, and the locus ceruleus, neurofibrillary tangles are frequently observed.

Electron microscopic studies show that paired helical filaments (PHF) are the main constituents of the neurofibrillary tangles found in cell bodies and in neurites. Each member of the pair is a filament about 10 nm in diameter. The pair of filaments measures about 22–24 nm at its maximum width, and the helical twist has a period of about 70–80 nm.

In GSS-198 and GSS-217, many nerve cell bodies are strongly immunolabeled by Alz50, a monoclonal antibody that recognizes a 68-kDa protein present in large amounts in AD brains. In most labeled neurons, the reaction product is circumscribed in a portion of the cytoplasm, which shows a globular or flame-shaped fibrillary appearance and contains neurofibrillary tangles. Anti-PHF, anti-PHF absorbed with τ and antiubiquitin antibodies also immunostain the neurofibrillary tangles.

All these antibodies reveal the neuritic component, which surrounds the amyloid deposits in the cerebral cortex. Moreover, Alz50 labels neuropil threads that are not spatially associated with amyloid deposits or neurofibrillary tangles, and are particularly abundant in the parahippocampal gyrus. Double anti-PrP/Alz50 and anti-SP28/Alz50 immunohistochemical staining clearly demonstrates that anti-PrP-positive and anti-SP28-negative amyloid deposits in the cerebral cortex are surrounded by Alz50-positive dystrophic neurites. With regard to the cerebellum, no immunolabeling with Alz50 and anti-PHF antibodies is detected around the amyloid deposits.

In particular, we have studied the antigenic profile of neurofibrillary tangles in GSS-198 by immunocytochemistry and immunoblot analysis using antibodies to various domains of the τ molecule *(21,25)*:

1. Alz50 to an epitope at the N-terminus;
2. τ-46 to an epitope at the C-terminus; and
3. τ-1 to an epitope in the midregion that is a phosphorylation site.

Since abnormal phosphorylation of τ prevents this epitope from being accessible to τ-1, some sections were dephosphorylated before immunostaining (*Escherichia coli* alkaline phosphatase type III, 25 U/mL, 16 h, 37°C).

Immunogold labeling with Alz50 and τ-46 was carried out following a pre-embedding procedure and using goat antimouse immunoglobulins conjugated with 10-nm colloidal gold particles. At the light microscopy level, it was observed that Alz50 and τ-46 labeled neurofibrillary tangles, degenerating neurites, and neuropil thread in all Alzheimer's patients and all GSS-198 patients as well. Immunostaining with τ-1 was observed in sections treated with alkaline phosphatase. By immunogold electron microscopy, it was found that Alz50 and τ-46 recognized intracellular PHF of GSS-198 patients and Alzheimer's patients.

PHF-enriched fractions were obtained from the frontal and temporal cortices of GSS-198 patients. These fractions, assessed for the presence of PHF by electron microscopy after negative staining with 2% uranyl acetate, were suspended in SDS-sample buffer, sonicated, and boiled. Proteins were separated on 10% SDS-polyacrylamide gels, electrophoretically transferred to PVDF membranes, and incubated with Alz50, τ-46, and τ-1 antibodies. In some experiments, immunostaining of the proteins transferred to PVDF membranes was preceded by dephosphorylation with *E. coli* alkaline phosphatase type III. Either alkaline phosphatase-conjugated goat antimouse IgG with BCIP/NBT as chromogen or horseradish peroxidase-conjugated sheep antimouse IgG with DAB as chromogen was used for immunodetection.

In negatively stained samples studied by electron microscopy, the ultrastructure of PHF obtained from the cerebral cortex of GSS patients is identical to that of PHF prepared by the same procedure from Alzheimer's patients. PHF-enriched fractions are only partially soluble in SDS-sample buffer. Alz50 and τ-46 immunostaining of proteins separated by SDS-PAGE and transferred to PVDF membranes identified three peptides migrating at 68, 64, and 60 kDa. Pretreatment of samples with alkaline phosphatase is ineffective on immunostaining with Alz50 or τ-46, but influences that with τ-1. The latter, in fact, labeled peptides migrating from 45 to 60 kDa and, after dephosphorylation, immunostained additional peptides migrating at 64 and 68 kDa.

It is possible to conclude that in affected members of GSS-198, the SDS-soluble fraction of PHF contains proteins with both electrophoretic mobility and immunochemical profile corresponding to those of A68 extracted from the brain of Alzheimer's patients. In AD and GSS-198, as well, these proteins migrate between 60 and 68 kDa, immunoreact with antibodies to the N and C terminus of τ, and require dephosphorylation to be accessible to τ-1. The immunocytochemical findings are consistent with those of the Western blot analysis showing that no difference exists between GSS-198 and

AD as to the Alz50, T46, and τ-1 immunostaining of neurofibrillary tangles. In conclusion, A68 is a component of neurofibrillary tangles in GSS-198 as it is of neurofibrillary tangles in AD.

Animal Transmission Studies

Inoculation of brain tissue from one GSS-198-affected individual into hamsters was carried out in the laboratory of E. Manuelidis in 1987, and no transmission has occurred. Tissue from one GSS-198 patient and one GSS-217 patient has been subsequently inoculated into hamsters and mice in S. Prusiner's laboratory, and no transmission had occurred more than 450 d after inoculation.

Molecular Genetics

PRNP Gene in GSS-198

DNA of affected patients from the Indiana kindred has been subjected to polymerase chain amplification of the PRNP open reading frame (ORF). Both total amplified product and individually subcloned amplified PrP ORFs have been sequenced. Some patients are heterozygous (met/val) for a normal intragenic variant at codon 129, thus enabling identification of both PrP alleles in those individuals. Other patients are homozygous (val/val) at codon 129. In all affected individuals sequenced, a thymine (T) to cytosine (C) transition has been found at codon 198 of one allele of the PrP ORF, resulting in a phenylalanine to serine substitution *(14,16)*. Allele-specific oligonucleotide hybridization has been used to demonstrate the presence of the mutation in all affected family members and, in addition, to identify asymptomatic gene carriers.

PRNP Gene in GSS-217

An adenine (A) to guanine (G) transition has been found at codon 217 of one allele of PRNP, resulting in a glutamine to arginine substitution. In one patient heterozygous (met/val) at codon 129, the mutation at codon 217 is associated with GTG valine at codon 129. In addition, a silent polymorphism has been discovered at codon 124 of the "normal" allele, the significance of which is unknown *(16)*.

Conclusion

The missense mutations found at codons 198 and 217 of PRNP are likely to be the disease-causing mutations. This conclusion for GSS-198 also is supported by a lod score of >7 ($\theta = 0$) obtained in genetic linkage analysis. How the mutations trigger amyloid deposition is unknown. Since in GSS-198 the amyloid is composed of an 11-kDa fragment of the full-length PrP, our findings suggest that the disease process leads to proteolytic cleavage of PrP 33–35, generating an amyloidogenic peptide that polymerizes into insoluble fibrils. However, it is interesting that the mutation lies outside the sequence that codes for the portion of PrP that was isolated as a major component of the amyloid. Thus, the exact relationship, if any, among the codon 198 mutation, PrP cleavage, and amyloid deposition must be elucidated. Also, it is tempting to speculate that the 198 and 217 mutations, alone or in combination with other factors, may have a significant role in the pathogenesis of neurofibrillary tangle formation.

In both GSS-198 and GSS-217, the putative disease-causing mutation is in coupling phase with valine at codon 129. Polymorphism at codon 129 has been implicated in the pathogenesis of a number of prion diseases. In GSS-198, patients who are heterozygous met/val at codon 129 appear to have a later age of onset (59 yr of age, $n = 8$) than patients who are val/val homozygotes (43.7 yr of age, $n = 3$) at codon 129. These data are consistent with the view that homozygosity at codon 129 predisposes to increased susceptibility, earlier age of onset, or earlier age of death in prion disease.

Acknowledgment

This work was supported in part by PHS R01-NS29822.

References

1. Gerstmann J., Sträussler E., and Scheinker I. (1936) *Z. Neurol.* **154,** 736–762.
2. Masters C. L., Gajdusek D. C., and Gibbs C. J., Jr. (1981) *Brain* **104,** 559–588.
3. Farlow M. R., Tagliavini F., Bugiani O., and Ghetti B. (1991) in *Handbook of Clinical Neurology: Hereditary Neuropathies and Spinocerebellar Atrophies,* vol. 16, no. 60 (Vinken P. J., Bruyn G. W., Klawans H. L., and deJong J. M. B. V., eds.), Elsevier, Amsterdam, pp. 619–633.
4. Bolton D. C., McKinley M. P., and Prusiner S. B. (1982) *Science* **218,** 1309–1311.
5. Goldgaber D., Goldfarb L. G., Brown P., Asher D. M., Brown W. T., Lin S., and Teener J. W. (1989) *Exper. Neurol.* **106,** 204–206.
6. Hsiao K., Baker H. F., Crow T. J., Poulter M., Owen F., Terwillinger J. D., Westaway D., Ott J., and Prusiner S. B. (1989) *Nature* **338,** 342–345.

7. Kretzchmar H. A., Honold G., Seitelberger F., Feuchd M., Wessely P., Mehraein P., and Budka H. (1991) *Lancet* **337,** 1160.
8. Brown P., Goldfarb L. G., Brown W. T., Goldgaber D., Rubenstein R., and Kascsak R. J. (1991) *Neurology* **41,** 375–379.
9. Kitamoto T., Ohta M., Doh-ura K., Hitoshi S., Terao Y., and Tateishi J. (1993) *Biochem. Biophys. Res. Comm.* **191,** 709–714.
10. Hsiao K. K., Cass C., Schellenberg G. D, Bird T., Devine-Gage E., Wisniewski H. M., and Prusiner S. B. (1991) *Neurology* **41,** 681–684.
11. Tranchant C., Doh-ura K., Steinmetz G., Chevalier Y., Kitamoto T., Tateishi J., and Warter J. M. (1991) *Rev. Neurol.* **147,** 274–278.
12. Tranchant C., Doh-ura K., Warter J. M., Steinmetz G., Chevalier Y., Hanauer A., Kitamoto T., and Tateishi J. (1992) *J. Neurol. Neurosurg. Psychiatry* **55,** 185–187.
13. Hsiao K. and Prusiner S. B. (1990) *Neurology* **40,** 1820–1827.
14. Dlouhy S. R., Hsiao K., Farlow, M. R., Foroud T., Conneally P. M., Johnson P., Prusiner S. B., Hodes M. E., and Ghetti B. (1992) *Nature Genetics* **1,** 64–67.
15. Ghetti B., Tagliavini F., Dlouhy S. R., Yee R. D., Giaccone G., Conneally P. M., Hodes M. E., Bugiani O., Prusiner S. B., Frangione B., and Farlow M. R. (1992) in *Prion Diseases of Humans and Animals* (Prusiner S., Collinge J., Powell J., and Anderton B., eds.), Ellis Horwood Limited, Chichester, England, pp. 154–167.
16. Hsiao K., Dlouhy S. R., Farlow M. R., Cass C., DaCosta M., Conneally P. M., Hodes, M. E., Ghetti B., and Prusiner S. B. (1992) *Nature Genetics* **1,** 68–71.
17. Ghetti B., Tagliavini F., Masters C. L., Beyreuther R., Giaccone G., Verga L., Farlow M. R., Conneally P. M., Dlouhy S. R., Azzarelli B., and Bugiani O. (1989) *Neurology* **39,** 1453–1461.
18. Ghetti B., Koo E. H., Farlow M. R., Dlouhy S. R., Giaccone G., Bugiani O., and Tagliavini F. (1993) *Neurology* **43(Suppl. 2),** A253.
19. Farlow M. R., Yee R. D., Dlouhy S. R., Conneally P. M., Azzarelli B., and Ghetti B. (1989) *Neurology* **39,** 1446–1452.
20. Yee R. D., Farlow M. R., Suzuki D. A., Betelak, K. F., and Ghetti B. (1992) *Arch. Ophthalmol.* **110,** 68–74.
21. Giaccone G., Tagliavini F., Verga L., Frangione B., Farlow M. R., Bugiani O., and Ghetti B. (1990) *Brain Res.* **530,** 325–329.
22. Giaccone G., Verga L., Bugiani O., Frangione B., Serban D., Prusiner S. B., Farlow M. R., Ghetti B., and Tagliavini F. (1992) *Proc. Natl. Acad. Sci. USA* **89,** 9349–9353.
23. Bugiani O., Giaccone G., Verga L., Pollo B., Frangione B., Farlow M. R., Tagliavini F., and Ghetti B. (1993) *J. Neuropathol. Exp. Neurol.* **52,** 64–70.
24. Tagliavini F., Prelli F., Ghiso J., Bugiani O., Serban D., Prusiner S. B., Farlow M. R., Ghetti B., and Frangione B. (1991) *EMBO J.* **10,** 513–519.
25. Tagliavini F., Giaccone G., Prelli F., Verga L., Porro M., Trojanowski J. Q., Farlow M. R., Frangione B., Ghetti B., and Bugiani O. (1993) *Brain Res.* **616,** 325–328.